

OPEN ACCESS

Suitability of the Hanging Meniscus RDE for the Electrochemical Investigation of Ionic Liquids

To cite this article: K. Wippermann et al 2020 J. Electrochem. Soc. 167 046511

View the <u>article online</u> for updates and enhancements.





Suitability of the Hanging Meniscus RDE for the Electrochemical Investigation of Ionic Liquids

K. Wippermann, D. Y. Suo, and C. Korte

Forschungszentrum Jülich GmbH, Institute of Energy and Climate Research, Electrochemical Process Engineering (IEK-14), 52425 Jülich, Germany

Employing the oxygen reduction reaction (ORR) exemplarily, the suitability of the hanging meniscus RDE (HMRDE) technique for viscous electrolytes—in particular for ionic liquids—was examined. RDE and HMRDE experiments were carried out using polycrystalline Pt disks in contact with either concentrated phosphoric acid, N,N-diethylmethylammoniumtriflate ([Dema][TfO]) or 2-sulfoethylmethyl-ammoniumtriflate ([2-Sema][TfO]). RDE measurements revealed Levich factors of the oxygen transport close to the theoretical value, even if the thickness of the hydrodynamic layer was about 33 of the disk diameter. HMRDE experiments showed a pronounced scattering of the Levich factors, which means a significant error in the determination of the mass transport parameters. In contrast, reliable Tafel factors of ORR were obtained from HMRDE experiments with viscous mixtures of [2-Sema] [TfO] and water. The thickness of the perturbed layer δ_{pl} near the edge of the HMRDE was found to be virtually independent of the viscosity of the respective electrolyte. In the case of viscous electrolytes like ionic liquids, the HMRDE technique is particularly suitable for investigating the kinetic parameters of electrochemical processes at elevated temperatures >100 °C, whereas a more precise determination of mass transport properties will only be possible once the experimental error can be significantly reduced. © 2020 The Author(s). Published on behalf of The Electrochemical Society by IOP Publishing Limited. This is an open access article distributed under the terms of the Creative Commons Attribution 4.0 License (CC BY, http://creativecommons.org/licenses/ by/4.0/), which permits unrestricted reuse of the work in any medium, provided the original work is properly cited. [DOI: 10.1149/ 1945-7111/ab75f9] **(i)**

Manuscript submitted December 4, 2019; revised manuscript received January 30, 2020. Published February 28, 2020.

Supplementary material for this article is available online

Hanging meniscus electrodes (HME) were originally developed for the electrochemical investigation of single crystals. The main reason for this was that the effective sealing of single crystals in mantles is difficult. The resulting gaps lead to unwanted leak currents and, typically, to a tilted baseline of the DC current. The first HME design and studies were published in 1976 by Dickertmann et al. 1 They brought the oriented side (111/100/110) of single crystals (Au/Ag) in contact with an electrolyte (1 M HClO4 $+\ 10^{-3} M\ Cu^{2+}/Pb^{2+})$ and then lifted the single crystal by a few mm to create a hanging meniscus of the electrolyte.

More than a decade later, Cahan and Villullas were the first to develop a hanging meniscus rotating disk electrode (HMRDE), combining the advantages of HMEs and rotating disc electrodes (RDEs). They used single crystal as well as polycrystalline Au electrodes and a $0.2\,\mathrm{M}$ Na₂SO₄ + $0.002\,\mathrm{M}$ ferri-/ferrocyanide electrolyte. The cylindrical electrodes were fixed with a miniature collet chuck mounted in KEL-F. The authors demonstrated the validity of the HMRDE method up to a rotational speed of $10,000\,\mathrm{rpm}$. The Levich plots of the cathodic limiting currents at different speeds revealed a linear slope, i.e., they matched the Levich equation. However, a negative intercept was obtained, which Cahan and Villullas referred to as the special hydrodynamic conditions of the HMRDE without providing a theoretical basis.

A few years later, the theoretical basis was established by Villullas and Lopez Teijelo^{5–7} and Villullas et al. in a series of four publications.⁸ They proposed modified Levich equations for the new hydrodynamic boundaries of the HMRDE, including simple charge transfer (CT) reactions,^{5,6} more complex CT reactions with a preceding chemical reaction⁷ and catalytic processes.⁸ A key point of this theory is the evidence of a reverse flow and a perturbed electrolyte layer near the disk edge, leading to a decrease in the diffusion current.⁵ This explains both the lower limiting current and the negative intercept in the Levich plots of HMRDEs compared to those of RDEs.

A common feature of all of the literature results mentioned above is that they were achieved by performing experiments on aqueous electrolytes. The same applies for more recent studies, where the HMRDE method in particular has been used for the study of

electrochemical processes on single crystals in aqueous solutions, e.g., the kinetics of the oxygen reduction reaction (ORR) on rotating Pt single crystal electrodes. ⁹⁻¹¹ One HMRDE study was conducted by Kroen et al., ¹² who used 50 wt% phosphoric acid as a concentrated electrolyte. Kroen et al. studied the ORR on polycrystalline Pt and compared the RDE and HMRDE measurements. In contrast to the RDE studies, the Levich plots yielded from the HMRDE experiments had a smaller slope than expected (constant = 0.48 instead of 0.62) and non-linear Tafel plots. Kroen et al. concluded that precise kinetic data could not be obtained by using the HMRDE method in its state at that time.

However, to the best of our knowledge, the HMRDE technique has never been used for the investigation of electrochemical processes on electrodes in ionic liquids. One of many possible applications of ionic liquids is their use as an alternative protonconducting electrolyte in polymer electrolyte fuel cells at elevated temperatures. Brønsted-acidic proton-conducting ionic liquids (PILs), such as 2-sulfoethylammonium trifluoromethanesulfonate ([2-Sea][TfO])¹³ and 2-sulfoethylmethylammonium trifluoromethanesulfonate ([2-Sema][TfO]), are promising candidates. 14,15 By means of stationary macro electrodes (e.g., Pt wires), the ionic conductivity, ^{13,15} electrochemical processes ^{13,15} such as the ORR, the H_{UPD} , the formation and reduction of PtO_x and double layer properties ¹⁴ were recently investigated. As reference electrolytes to compare the performance, concentrated phosphoric acid as the stateof-the-art electrolyte in HT-PEFCs and [Dema][TfO] (N,N-diethylmethylammoinum trifluoromethanesulfonate) as a commerciallyavailable ionic liquid are used. [Dema][TfO] has also been proposed as an proton-conducting ionic liquid for use in fuel cells. 16 The molecular structures of [2-Sea][TfO], [2-Sema][TfO] and [Dema] [TfO] are depicted in Fig. 1.

The oxygen reduction reaction on electrodes in ionic liquids has been studied by using stationary macro electrodes, $^{13,17-22}$ rotating disk $^{23-28}$ or ring disk $^{26,29-31}$ electrodes and micro electrodes. Recently, an overview of ORR on electrodes in ILs was given by Khan et al. Because of the fast mass transport, the limiting ORR current on rotating disk electrodes and micro electrodes is much higher compared to stationary macro electrodes. This allows the analysis of the ORR kinetics over a larger potential range, e.g., the rate of mass transport at a micro electrode with a diameter of 10 μ m is comparable with that of an RDE rotating at

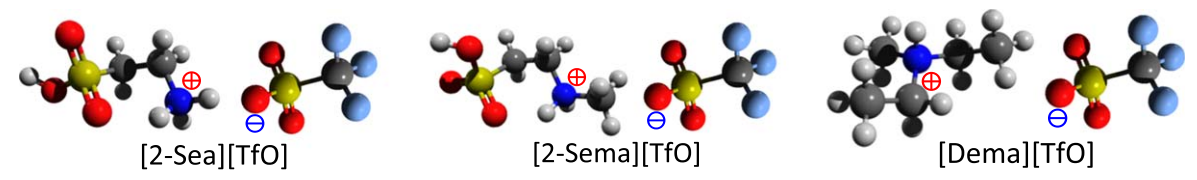


Figure 1. Molecular structure of the ionic liquids [2-Sea][TfO], [2-Sema][TfO] and [Dema][TfO].

4000 rpm. ⁴¹ As is the case for RDEs and all other kinds of embedded or mantled electrodes, micro electrodes are subject to the risk of leakage. ⁴² Moreover, they are prone to poisoning effects and the mantle material (e.g., soft glass, epoxy resin, etc.) may be attacked by corrosive electrolytes, ⁴³ such as hot, concentrated phosphoric acid or HF and HF-liberating compounds.

As already mentioned, HMRD electrodes do not need to be sealed. This is not only a major advantage for the investigation of single crystals in aqueous solutions at moderate temperatures (25 °C–100 °C), but is also useful for studies of polycrystalline electrodes at elevated temperatures (100 °C–200 °C) in highly concentrated solutions, in particular ionic liquids. Under these conditions, common RDEs fail because the mismatch of the expansion coefficients of the electrode material (metal, glassy carbon, etc.) and the mantle (PTFE, PEEK, etc.) causes electrolyte leakages and the issues discussed above. This problem may also arise with micro electrodes. The leaking effect is further enhanced by increasing the rotation rate and temperature. Up to temperatures of 130 °C–150 °C, technical solutions like putting pressure on the mantle⁴⁴ or reinforcing it by a steel ring⁴⁵ have been used, but they require high instrumental efforts and have not yet been established.

Thus, it appears obvious to use HMRDEs at elevated temperatures, particularly in the temperature range above 150 °C. However, concentrated electrolytes in general and ionic liquids in particular have the drawback of possessing viscosities several orders of magnitude higher compared to those in aqueous electrolytes. ¹³ For both RDE and HMRDE measurements, high viscosities may change the hydrodynamic pattern and violate basic conditions of the Levich equation. First, a detailed discussion of the theoretical limits of viscosity and the consequences of high viscosities will be presented in this article. A special, often related problem of many ionic liquids is their high viscosity in combination with very low diffusion coefficients and concentrations of oxygen, which requires high rotation rates to achieve a steady state. ⁴⁶

The aim of this work is to evaluate the suitability of the HMRDE technique for the study of electrochemical processes at the electrode/ionic liquid interface. For this, proton-conducting ionic liquids with small amounts of water, namely [2-Sema][TfO] and [Dema][TfO], were chosen. The oxygen reduction reaction (ORR) on polycrystal-line Pt electrodes (HMRDE/RDE) is also investigated. The results are compared with those obtained from concentrated phosphoric acid and literature data from aqueous electrolytes. By varying the type of electrolyte, water content and operating temperature, a viscosity range of about five orders of magnitude is covered. A special focus is on the HMRDE measurements of oxygen transport and ORR kinetics. The validity of the Levich equation and the reliability of the resulting Tafel slopes are also verified.

Application of RDEs for Highly Viscous Electrolytes

General considerations.—In low viscosity fluids like aqueous electrolytes, anomalies at the disk edge such as enhanced current densities ⁴⁷ or distortions of the electrolyte flow pattern ⁴⁸ (hereinafter referred to as "edge effects"), are usually neglected. In this case, the limiting current i_{lim,RDE} of mass transport, controlled electrochemical processes, obeys the Levich equation ⁴⁹:

$$i_{\text{lim,RDE}} = 0.62 \, n \, F \, D^{\frac{2}{3}} \, \omega^{\frac{1}{2}} \, \nu^{-\frac{1}{6}} \, C_0 \, \pi r_0^2$$
 [1]

Here, D and C_0 are the bulk diffusion coefficients and bulk concentration of the electrochemical active species, ω is the angular rotation rate of the disk, ν is the kinematic viscosity of the electrolyte and r_0 the disk radius.

The importance of edge effects can be demonstrated by means of two parameters: the thickness of the hydrodynamic boundary layer δ_h (also known as Prandtl's boundary layer), and the Reynolds number Re. For Newtonian fluids, an approximate value of δ_h was provided by Levich⁴⁹:

$$\delta_{\rm h} = 3.6 \left(\frac{\nu}{\omega}\right)^{0.5}$$
 [2]

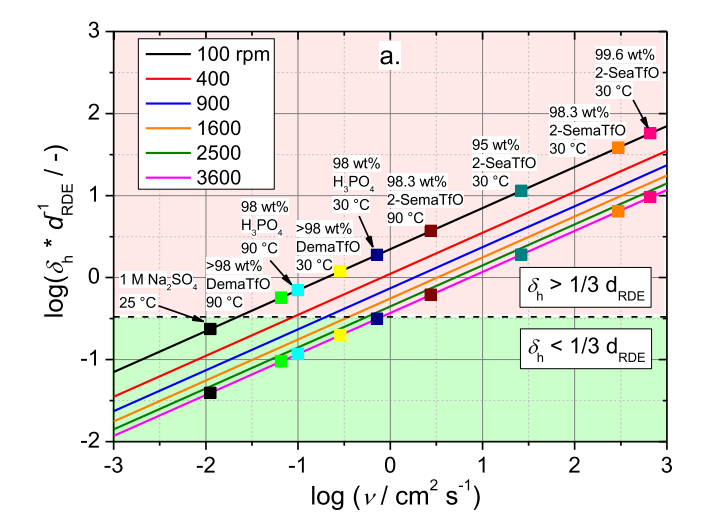
It is important to note that viscous ionic liquids in particular may exhibit non-Newtonian behavior and thus Eq. 2 may no longer be valid. Following Legrand et al., 50 edge effects must be considered if the thickness of the hydrodynamic layer is equal to (or even higher than) $\frac{1}{3}$ of the disk diameter d:

$$\delta_{\rm h} \geqslant \delta_{\rm h,crit} = \frac{1}{3} d_{\rm RDE}$$
 [3]

A useful graph is shown in Fig. 2a, where the (dimensionless) ratio of $\delta_{\rm h}$ and d is plotted against the kinematic viscosity of different electrolytes on a double logarithmic scale. A disk diameter d=0.5 cm was chosen because all of the HMRDE and most of the RDE experiments were performed with this geometry (see "experimental part"). Dividing Eq. 2 by d, linear plots of $\log(\delta_{\rm h}/d)$ vs $\log\nu$ with a slope of 0.5 must result. The intercept = $\log(3.6/d) - 0.5\log\omega$ decreases with an increasing rotation rate. The full lines in Fig. 2a show plots for a typical speed range of 100-3600 rpm. Additionally, the points denote the values for six electrolytes with different water contents and for different temperatures (25 °C, 30 °C and 90 °C) and rotation rates (100 and 3600 rpm). The broken line corresponds to $\delta_{\rm h}/d = \frac{1}{3}$ and divides the diagram into an upper, critical area (red) and a lower, noncritical area (green). If $\delta_{\rm h}/d > \frac{1}{3}$, edge effects should be taken into account and the Levich equation may no longer be valid.

Obviously, the critical kinematic viscosity that corresponds to $\delta_{\rm h}/d=1/3$ depends on the rotational speed of the RDE (see the intersection points of the graphs and the broken line). If the lowest rpm value of 100 is not considered, it can be concluded that kinematic viscosities of about 0.1–1 cm² s⁻¹ should not be exceeded to avoid edge effects. As can be seen from Fig. 2, only 1 M Na₂SO₄ solution and, at sufficiently high temperatures and rotation rates, [Dema][TfO] and 98 wt% H₃PO₄, fulfil this criterion. In contrast, high $\delta_{\rm h}/d$ values of up to 50 are reached in the case of highly viscous ionic liquids like [2-Sea][TfO] and [2-Sema][TfO]. Taking a disk diameter of 0.5 cm into account, this would correspond to a theoretical $\delta_{\rm h}$ value of 25 cm. If one considers the usual vessel dimensions in the range of a few cm, the hydrodynamic boundary layer could not be (fully) established.

The Reynolds number is another parameter that depends on the viscosity of the fluids⁵¹ (see Eq. 4) and allows the evaluation of critical viscosities as well. Re is proportional to the square of the disc radius and inversely proportional to the kinematic viscosity:



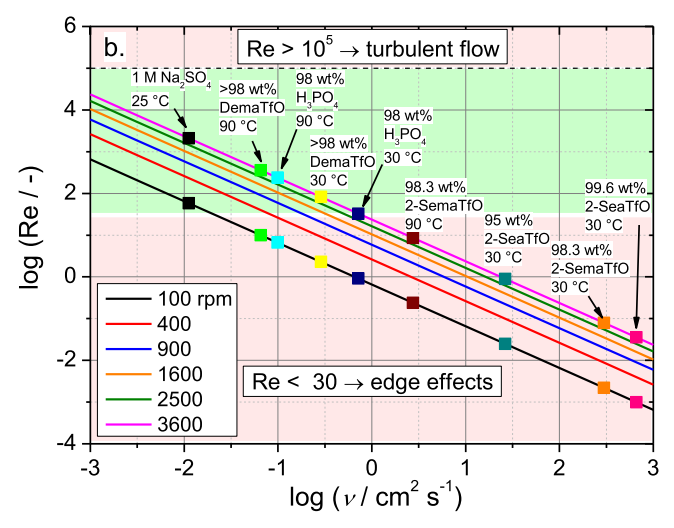


Figure 2. Plots of $\log(\delta_h/d)$ vs $\log \nu$ (a) and Re vs $\log \nu$ (b), showing noncritical (green) and critical (red) regions; the solid lines denote $\log(\delta_h/d)$ and Re values for six different rotation rates, calculated from Eqs. 2 and 4; the squares mark the values for six electrolytes at different water contents, temperatures, kinematic viscosities and rotation rates; the corresponding values of ν , δ_h/d and Re are listed in Table I.

$$Re = \frac{r^2 \omega}{V}$$
 [4]

According to Legrand et al.,⁵⁰ the critical Reynolds number that should not be undercut is 30 and is valid for both Newtonian and non-Newtonian fluids. Combining Eqs. 2 to 4, one obtains the following links between δ_h and Re, as well as $\delta_{h,crit}$ and Re_{crit}:

$$\delta_{\rm h} = 3.6 \, r \, Re^{-0.5}$$
 [5a]

$$\delta_{\text{h.crit}} = 3.6 \ r \ Re_{\text{crit}}^{-0.5} = 3.6 \ r \ 30^{-0.5} = 0.66 \ r = 0.33 \ d$$
 [5b]

Thus, it is not surprising that the double logarithmic plot of Re vs kinematic viscosity ν shown in Fig. 2b yields the same critical values for the viscosities as the corresponding values estimated from Fig. 2a (see the intersection points of the graphs with the broken line at Re = 30). Table I summarizes the δ_h/d_{RDE} values and Reynolds numbers obtained for different electrolytes, temperatures and rotational speeds. The calculations are based on the Eqs. 2 to 4. The type of Pt electrode (RDE or HMRDE) is also indicated. In this case, the values were calculated for the lower and upper limit of the

experimental rotation rate. If no RDE or HMRDE measurement was performed, rotation rates of 100 and 3600 rpm were used. For the RDE and HMRDE experiments, Re and $\delta_{\rm h}/d_{\rm RDE}$ values within the critical regions, where edge effects are expected, are shown in bold.

Because RDE experiments are usually performed at maximum rotation rates of several thousand rpm, none of the electrolytes shown in Fig. 2 should be prone to turbulent flow, particularly not the highly viscous ILs, cf. Eq. 4. Nevertheless, turbulence, even in ionic liquids (PYR14TFSI and PYR1(2O1)TFSI), has been reported at much lower critical Reynolds numbers of 40–50, compared to the theoretical value of 10⁵.²³ Possible reasons are discussed in the first section of the Supplementary Material (available online at stacks.iop.org/JES/167/046511/mmedia). Other problems caused at high viscosities include a significantly increased transient time to reach steady state conditions, ⁵⁷ i.e., possibly an incompletely developed velocity field. ⁵⁸ For the above-mentioned reasons, severe problems can arise when using RDEs for viscous electrolytes and it is questionable if the Levich equation would remain valid.

Specific issues of HMRDEs.—If RDEs in general have an edge problem under certain operating conditions and have unfavorable material properties, this issue is intrinsic to HMRDEs under any conditions: As mentioned above, there is a reverse flow close to the disk edge. Figure 3 shows a schematic drawing of the electrolyte flow at the disk for two different meniscus heights. In the left part, specific parameters of the HMRDE are indicated for a proper meniscus height. The scheme on the right side shows lateral wetting of the HMRDE in the case of too small a meniscus height. Cahan and Villullas defined a critical meniscus height h_0 that should not be undercut. If this condition is fulfilled, the thickness $\delta_{\rm pl}$ of the perturbed layer at the edge can be simply subtracted from the disk radius to obtain an effective, reduced value of the disk radius and thus the electrode area. The calculation of the effective radius starts from the assumption that δ_{pl} is in the same order of magnitude compared to the thickness δ_h of the hydrodynamic boundary layer. On basis of the effective disk radius, Cahan proposed a modified Levich equation for HMRDEs:5

$$i_{\text{lim,HMRDE}} = 0.62 \, n \, F \, D^{-\frac{2}{3}} \, \omega^{\frac{1}{2}} \, \nu^{-\frac{1}{6}} \, C_0 \, \pi r_0^2$$

$$\times \left[1 - \left(2 \, K \, r_0^{-1} \left(\frac{\nu}{\omega} \right)^{\frac{1}{2}} \right) \right]$$
 [6a]

$$slope_{\rm HMRDE} = slope_{\rm RDE} = 0.62 \, n \, F \, D^{\frac{2}{3}} \, \nu^{-\frac{1}{6}} \, C_0 \, \pi r_0^2$$
 [6b]

$$intercept_{\text{HMRDE}} = -1.24 \, n \, F \, D^{\frac{2}{3}} \, \nu^{\frac{1}{3}} \, C_0 \, \pi r_0 \, K$$
 [6c]

$$K = -\frac{intercept_{\text{HMRDE}}}{slope_{\text{HMRDE}} \times 2 \nu^{\frac{1}{2}} r_0^{-1}}$$
 [6d]

Here, K is a dimensionless proportionality factor and $K^*(\nu/\omega)^{0.5}$ equals $\delta_{\rm pl}$. A comparison of the Eqs. 1 and 6a–6c shows, that Levich plots of RDE and HMRDE measurements yield identical slopes but different intercepts, i.e. zero intercepts for RDEs and negative intercepts in case of HMRDEs. Modified Levich equations for more complex reactions at HMRDEs are beyond the scope of this study, and will not be further discussed here. ^{7,8} A brief overview of the theory of Cahan and Villullas including a detailed description of the calculation of $r_{\rm eff}$, K and $i_{\rm lim, HMRDE}$ can be found in the second section of the Supplementary Material (available online at stacks. iop.org/JES/167/046511/mmedia).

Based on the theoretical analysis and experimental work of Cahan and Villullas et al., it turns out that the modified Levich equation presented in Eq. 6a describes the behavior of HMRDEs in

Table I. Values of δ_b/d_{RDE} and Reynolds numbers calculated from the dynamic viscosities and densities of different electrolytes and for different rotation rates; in the case of DemaTfO and phosphoric acid, literature data were used: the η values were taken from earlier studies⁵² (DemaTfO) and 53,54 (H₃PO₄), and the ρ values from more recent ones⁵⁵ (DemaTfO) and 56 (H₃PO₄); the type of electrode (HMRDE or RDE) is indicated; if not, no electrochemical measurement was performed; the critical δ_b/d_{RDE} and Re values are shown in bold.

Pt electrode	electrolyte	T/°C	$v/\text{cm}^2\text{s}^{-1}$	rpm/min ^{−1}	$\delta_{ m h/cm}$	$\delta_{\rm h}^{*} { m d}^{-1}_{\rm RDE}$ /-	Re/-	rpm _{crit} /min ^{−1}
_	99.6 wt%	30	6.64×10^{2}	100	2.87×10^{1}	5.73×10^{1}	9.86×10^{-4}	2.96×10^{6}
	2-SeaTfO			3600	4.78×10^{-1}	$9.55 \times 10^{\circ}$	3.55×10^{-2}	
_	95.0 wt%	30	2.64×10^{1}	100	5.72×10^{0}	1.14×10^{1}	2.48×10^{-2}	1.18×10^{5}
	2-SeaTfO			3600	9.53×10^{-1}	1.91×10^{0}	8.92×10^{-1}	
				100	1.92×10^{1}	3.84×10^{1}	2.19×10^{-3}	1.33×10^{6}
_	98.3 wt%	30	2.98×10^{2}	3600	3.20×10^{0}	6.40×10^{0}	7.90×10^{-2}	
	2-Seama TfO			625	7.37×10^{-1}	1.47×10^{0}	1.49×10^{0}	1.22×10^4
HMRDE		90	2.74×10^{0}	2025	4.09×10^{-1}	8.19×10^{-1}	4.83×10^{0}	
HMRDE	95.4 wt%	90	5.50×10^{-1}	625	3.30×10^{-1}	6.60×10^{-1}	7.44×10^{0}	2451
	2-SemaTfO			2025	1.83×10^{-1}	3.67×10^{-1}	2.41×10^{1}	
HMRDE	95.6 wt%	90	6.19×10^{-1}	625	3.50×10^{-1}	7.00×10^{-1}	6.60×10^{0}	2759
	2-SemaTfO			2025	1.95×10^{-1}	3.89×10^{-1}	2.14×10^{1}	
HMRDE	95.9 wt%	90	7.05×10^{-1}	625	3.74×10^{-1}	7.47×10^{-1}	5.80×10^{0}	3141
	2-SemaTfO			2025	2.08×10^{-1}	4.15×10^{-1}	1.88×10^{-1}	
HMRDE	96.9 wt%	90	1.18×10^{0}	625	4.83×10^{-1}	9.66×10^{-1}	3.47×10^{0}	5246
	2-SemaTfO			2025	2.68×10^{-1}	5.37×10^{-1}	1.13×10^{1}	
HMRDE	97.7 wt%	90	1.75×10^{0}	625	5.89×10^{-1}	1.18×10^{0}	2.33×10^{0}	7819
	2-SemaTfO			2025	3.27×10^{-1}	6.55×10^{-1}	7.55×10^{0}	
RDE		70	6.24×10^{0}	625	1.11×10^{0}	2.22×10^{0}	6.55×10^{-1}	2.78×10^{4}
	97.9 wt%			2025	6.18×10^{-1}	1.24×10^{0}	2.12×10^{0}	
HMRDE	2-SemaTfO			625	6.13×10^{-1}	1.23×10^{0}	2.16×10^{0}	8442
		90	1.89×10^{0}	2025	3.40×10^{-1}	6.81×10^{-1}	6.99×10^{0}	
				225	3.97×10^{-1}	7.95×10^{-1}	5.13×10^{0}	
RDE	≈100 wt%	30	2.87×10^{-1}	1225	1.70×10^{-1}	3.41×10^{-1}	2.79×10^{1}	1279
	DemaTfO			100	2.85×10^{-1}	5.70×10^{-1}	9.97×10^{0}	
_		90	6.56×10^{-2}	3600	4.75×10^{-2}	9.50×10^{-2}	3.59×10^{2}	292
				100	1.05×10^{0}	2.10×10^{0}	7.34×10^{-1}	
RDE		25	8.92×10^{-1}	3600	1.75×10^{-1}	3.50×10^{-1}	2.64×10^{1}	3973
				100	9.44×10^{-1}	1.89×10^{0}	9.09×10^{-1}	
_		30	7.20×10^{-1}	3600	1.57×10^{-1}	3.15×10^{-1}	3.27×10^{1}	3208
	98 wt%			100	4.51×10^{-1}	9.02×10^{-1}	3.99×10^{0}	
RDE	H_3PO_4	75	1.64×10^{-1}	3600	7.51×10^{-2}	1.50×10^{-1}	1.43×10^{2}	732
				100	3.50×10^{-1}	7.01×10^{-1}	6.60×10^{0}	
		90	9.92×10^{-2}	3600	5.84×10^{-2}	1.17×10^{-1}	2.37×10^{2}	442
				900	6.77×10^{-2}	1.35×10^{-1}	1.77×10^{2}	
RDE,HMRDE	50 wt%	25	3.33×10^{-2}	3600	3.39×10^{-2}	6.77×10^{-1}	7.07×10^{2}	149
•	H_3PO_4			400	5.89×10^{-2}	1.18×10^{-1}	2.33×10^{2}	
RDE,HMRDE	1 M Na ₂ SO ₄	25	1.12×10^{-2}	8100	1.31×10^{-2}	2.62×10^{-2}	4.72×10^{3}	50

aqueous solutions satisfactorily. However, Cahan's assumption of comparable thicknesses of the perturbed layer and the hydrodynamic boundary layer is not valid for highly viscous electrolytes. In this case, the thickness of the perturbed layer would exceed the disk diameter, and so there will be a reverse flow over the entire disk area. In order to investigate this contradiction and evaluate the applicability of Eq. 6a, also for viscous electrolytes, appropriate HMRDE experiments were carried out (see "Results"). In view of the intrinsic edge effect of HMRDEs, another interesting aspect is the question of the edge effect proposed for RDEs and the corresponding critical limits that would also be valid for HMRDEs.

Experimental

Materials.—*Electrolytes.*—The electrolytes were prepared by reacting an organic base and triflic acid ([2-Sea][TfO] and [2-Sema] [TfO]), purchased from IoLiTec (>98 wt% [Dema][TfO]) and Merck KGaA (85 wt% H₃PO₄, Suprapur°), respectively. As organic bases, either taurine or N-methyltaurine were used (both $\ge 99\%$, Sigma Life Science). The reagent grade (98%) triflic acid was purchased from Sigma Aldrich. The strongly hygroscopic ionic liquids [2-Sea][TfO] and [2-Sema][TfO] have a minimum water content of 0.5 wt% after

preparation, whereas that of [Dema][TfO] was about 4000 ppm. Details concerning the preparation of [2-Sea][TfO] and [2-Sema] [TfO] can be found in previous studies. 13,14 If the water content must be modified, an appropriate amount of deionized water was added. In the case of 85 wt% $\rm H_3PO_4$, it was dried at 160 °C in an oven to yield a final concentration of 98 wt%. The water content of the prepared electrolytes was controlled by coulometric Karl-Fischer titration (852 Titrando, Metrohm GmbH & Co. KG).

Measuring vessels.—The measuring vessels for the RDE and HMRDE experiments were either a small cylindrical Pt crucible with an electrolyte volume of 3–4 ml (for details, see Wippermann et al.¹³) or a glass cell with a filling volume of about 100 ml. The Pt vessel was also used for coulometric measurements with microelectrodes.

Electrodes.—The RDEs and HMRDE were purchased from Pine Research Instrumentation. Pt disks with diameters of 5 mm (HMRDE) or 3 and 5 mm (RDEs) were used. The Pt disks of the RDEs were surrounded by either a PTFE ($T \le 30$ °C) or a PEEK ($T \le 80$ °C) mantle. The smaller RDE was primarily used for experiments with ionic liquids in the Pt vessel. The HMRDE disk had a thickness of about 1.2 mm and was mounted on a stainless

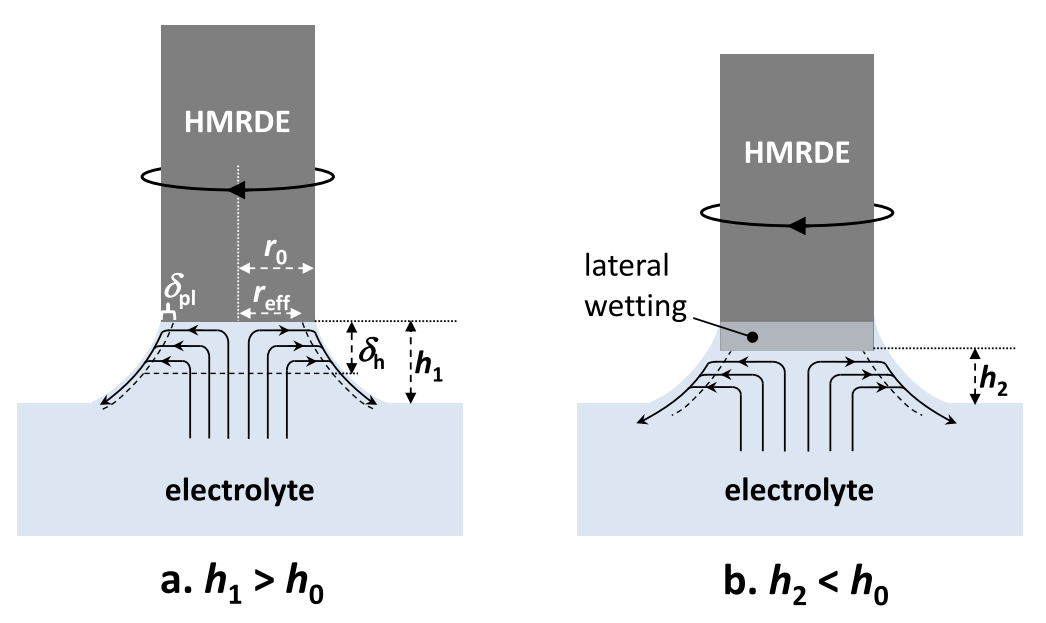


Figure 3. Schematic drawing of the flow conditions in the hanging meniscus under the disk surface and specific HMRDE parameters; left part: proper meniscus height $h_1 > h_0$; right part: too small a meniscus height $h_2 < h_0$ causing lateral wetting.

steel shaft. Prior to the electrochemical experiments, the disk electrodes were polished with $0.05~\mu m$ Al_2O_3 powder and thoroughly rinsed with Milli-Q * water. For the glass cell, a Pt sheet was used as a counter electrode (CE). This was not necessary for the small cell, because the Pt vessel itself served as the CE. The glass cell was equipped with a Gaskatel "HydroFlex * " hydrogen reference electrode. A Pd/H $_2$ reference electrode 13 was used for the Pt vessel.

A home-made microelectrode with a geometric area of $4.9 \times 10^{-4} \, \mathrm{cm}^2$ was prepared by fusing a 250 $\mu \mathrm{m}$ -thick Pt wire (Heraeus, 99.9%) into Schott AG-Glas* glass (soft glass). The microelectrode was used for the determination of the bulk diffusion coefficients and the concentrations of oxygen by means of chronoamperometric measurements.

Instrumentation and operating conditions.—A "Zennium" electrochemical workstation (ZAHNER Elektrik GmbH) was used to carry out quasi-stationary *U/I* and chronoamperometric measurements. The experiments were performed in a temperature range of 25 °C–90 °C and under ambient pressure. The temperature of the Pt crucible was controlled by a heating unit, as described in Wippermann et al. ¹³ A Haake B3-DC3 heating circulator was used for setting the temperature of the glass cell. In order to achieve oxygen saturation, the gas compartment over the electrolyte was purged with 99.998% dry oxygen. The oxygen supply was started one hour prior to the experiments and maintained until the end of the measurement process. The flow rate was 5–10 ml min⁻¹ in the case of the Pt crucible and 50–100 ml min⁻¹ for the glass vessel. It was adjusted by means of Brooks 5850S mass flow controllers.

The rotating disk experiments were carried out by means of an AFMSRCE Pine Modulated Speed Rotator. The minimum and maximum rotational speeds were 100 and 3600 rpm, respectively. Within this range, an appropriate rpm window was chosen for each measuring system. The meniscus height of the HMRDE was controlled by increasingly lowering the electrode in steps of 50–500 μ m, until contact was made with the electrolyte. If this was the case, a perfect sinusoidal a.c. signal was obtained in the impedance operating mode. Then, the HMRDE was lifted by a defined distance to attain the required meniscus with a typical height of $h\approx 2$ mm. In some cases, the HMRDE measurements were performed at various meniscus heights in order to evaluate critical meniscus heights, h_0 (see section 2). In the case of phosphoric acid/water and [2-Sema][TfO]/water mixtures, the potential of the Pd/H electrode was measured against a reference hydrogen electrode

(see, e.g., Wippermann et al.¹³), and so the electrode potentials are reported against RHE. For the other electrolytes, the potentials were quoted against the Pd/H reference electrode.

For the chronoamperometric measurements with micro electrodes, a Zahner "HiZ probe" (high impedance probe) was used to minimize electrical noise. The chronoamperometric experiments were performed by jumping from the OCV to an electrode potential in the limiting current range. The resulting *ilt*-curves were analyzed by using the equation of Shoup and Szabo⁵⁹ to obtain the diffusion coefficients and concentrations of oxygen in [Dema][TfO] and [2-Sema][TfO].

Results and Discussion

In the following, exemplary results of the RDE and HMRDE measurements with different electrolytes are shown. For each electrolyte, the $\emph{U/I}$ curves of the ORR were measured at different rotation rates. The limiting current densities of the ORR were plotted vs $\omega^{0.5}$ ("Levich plot"). In the case of HMRDE experiments, the Levich plots were corrected according to the Eqs. 6a–6c. As mentioned above, the HMRDE studies of Kroen et al. 12 revealed a reduced slope of the Levich plot with a factor of 0.48 instead of 0.62; see Eq. 1. Hereinafter, this experimentally-discovered factor will be referred to as the "Levich factor" or, simply, "LF". The Levich factors were calculated from the Levich plots as follows:

$$LF = \frac{slope}{4 F D_{0}^{\frac{2}{3}}, \nu^{-\frac{1}{6}} C_{O_2} \pi r_0^2}$$
 [7]

The slopes were taken from the linear fits of the corresponding Levich plots. The total number of transferred electrons in the ORR was set to 4. The latter value is justified, as the formation of water by a 4-electron ORR mechanism usually predominates on Pt electrodes in acidic solutions. A 4-electron mechanism has not only been confirmed for aqueous electrolytes, but also for concentrated phosphoric acid⁶⁰ and [Dema][TfO].³⁰ Our first studies of ORR kinetics on Pt electrodes in [2-Sema][TfO] yielded the same result.⁶¹ However, a small percentage of H₂O₂ formation cannot be excluded. This would lead to a total number of transferred electrons slightly smaller than 4 and to somewhat smaller values of the limiting currents of the slopes of the Levich plots and thus of the LFs. An inaccurate determination of the bulk parameter of the electrolytes would also influence the calculated LFs. This is especially true for

parameters with exponents of 1 and 2/3, i.e., $c_{\rm O2}$ and $D_{\rm O2}$, whereas inaccuracies of the kinematic viscosity ν with an exponent of -1/6 only have little influence. In any case, the above-mentioned effects must be taken into account when deciding whether the Levich equation is valid or not, i.e., if there is a small or large deviation of the calculated LFs from the theoretical value of 0.62. The Levich factors and the $D_{\rm O2}$ and $c_{\rm O2}$ values are summarized in Table II.

RDE and HMRDE experiments.—The Levich plots of three RDE measurements with concentrated electrolytes, namely 98 wt% $\rm H_3PO_4$, [Dema][TfO] and 97.9 wt% [2-Sema][TfO], are presented exemplarily in Figs. 4a and 4c. The corresponding $\it UII$ curves are shown as insets, with the individual rpm ranges chosen in such a way that only those rotation rates were considered where almost equidistant limiting currents i_{lim} were obtained. There is a linear change of i_{lim} with the square root of the rotation rate $\omega^{-1/2}$, resulting in fairly linear Levich plots. In the case of the less viscous $\rm H_3PO_4$ and [Dema][TfO] electrolytes, the calculated LFs of 0.64 and 0.60 are close to 0.62, whereas the higher viscous [2-Sema][TfO] yields an LF of only 0.55, which is about 11% lower than the theoretical value. These results are in accordance with the study by Legrand et al., 50 who also found a decrease in the LF if the Reynolds number Re is below a critical limit of 30, which applies to highly viscous electrolytes.

For each electrolyte and indicated temperature, a critical value $\omega_{\rm crit}$ of the rotational speed can be calculated. Below this value, edge effects must be considered. An overview of the critical rotation rates can be found in Table I. The calculation is done by setting $\delta_{\rm h} = \delta_{\rm h,crit}$ and combining Eqs. 2 and 3. In this case, the angular rotation rate has the meaning of a critical, minimum value that must not be undercut. From the experimenter's perspective, it is useful to calculate $rpm_{\rm crit}$ instead of $\omega_{\rm crit}$ values:

$$\frac{1}{3}d_{\text{RDE}} = \delta_{\text{h,crit}} = 3.6 \left(\frac{\nu}{\omega}\right)^{0.5} = 3.6 \ \nu^{0.5} 2\pi^{-0.5} rpm_{\text{crit}}^{-0.5} 60^{0.5} \quad [8a]$$

$$rpm_{crit} = \frac{3^2 \times 3.6^2 \times 60 \times \nu}{2\pi \times d_{RDE}^2} \approx \frac{1114 \,\nu}{d_{RDE}^2}$$
 [8b]

The rpm_{crit} values for the examples shown in Figs. 4a–4c (and Table I) are about 730 rpm (98 wt% H₃PO₄, 75 °C), 1280 rpm (>98 wt% [Dema][TfO], 30 °C) and 27800 rpm (97.9 wt% [2-Sema][TfO], 70 °C). In the case of H₃PO₄, only part of the experimental rpm values are lower than rpm_{crit} , whereas for the ionic liquids, all of the rpm values used in the experiments are situated below the critical value. This is especially true for 97.9 wt% [2-Sema][TfO], where the upper experimental rpm limit is more than one order of magnitude smaller than rpm_{crit} . The results suggest that the measured limiting currents and their dependence on the rotational speed are close to the values predicted by the Levich equation if rpm_{crit} is somewhat higher than the highest rotation rate used in the experiments. Only in the case of highly viscous ionic liquids like [2-Sema][TfO] at 70 °C do edge effects provoke larger discrepancies and the Levich factor tends to decline. ⁵⁰

As explained above, according to the works of Cahan and Villullas, HMRDEs show intrinsic edge effects that can be fully corrected by adding the absolute value of the (negative) intercept. In Fig. 4d, a typical result for HMRDE measurements with [2-Sema] [TfO]/water mixtures is depicted (here: 2.1 wt% of water). This experiment was carried out at 90 °C and a meniscus height of 2.18 mm. The fairly linear Levich plot yields an LF of 0.51, which is about 18% smaller than the theoretical value, but lower than the value obtained from the above-mentioned RDE experiment with the same, but more viscous electrolyte at lower temperature (LF = 0.55). This result is astonishing, as one would expect an LF closer to the theoretical value if the viscosity of the electrolyte is lower. An explanation will be given in the next section.

Levich factors in correspondence with the viscosity of the electrolytes.—Figure 5 shows a plot of the calculated LFs vs the logarithm of the kinematic viscosity. The green and red areas correspond to non-critical and critical ranges of the viscosity, as explained above. The transitional region marked in yellow corresponds to either critical or non-critical viscosities, depending on the rotational speed of the disk electrode. The black squares represent LF values obtained from RDE experiments, while those of HMRDE measurements are marked by red circles. Finally, the type of

Table II. Levich factors calculated from the Levich equation for the electrolytes are shown in Fig. 5; the calculation is based on the $D_{\rm O2}$ and $c_{\rm O2}$ values shown in this table, the dynamic viscosities listed in Table I and the total number of transferred electrons of 4; the superscript numbers denote the references for the literature data.

Pt Electrode	electrolyte	T/°C	$\mathrm{D}_{\mathrm{O}2}/\mathrm{cm}^2\mathrm{s}^{-1}$	Co ₂ /mol cm ⁻³	LF/-
HMRDE	95.4 wt%	90	3.21×10^{-6}	1.18×10^{-6}	0.47
	2-SemaTFO				
HMRDE	95.6 wt%	90	3.13×10^{-6}	1.18×10^{-6}	0.56
	2-SemaTfO				
HMRDE	95.9 wt%	90	3.06×10^{-6}	1.19×10^{-6}	0.56
	2-SemaTfO				
HMRDE	96.9 wt%	90	2.77×10^{-6}	1.20×10^{-6}	0.68
	2-SemaTfO				
HMRDE	97.7 wt%	90	2.59×10^{-6}	1.22×10^{-6}	0.48
	2-SemaTfO				
RDE	97.9 wt%	70	1.60×10^{-6}	9.13×10^{-7}	0.55
HMRDE	2-SemaTfO	90	2.56×10^{-6}	1.22×10^{-6}	0.51
			1.27×10^{-5}	1.75×10^{-6}	0.38^{62}
RDE	≈100 wt%	30	4.64×10^{-6}	1.97×10^{-6}	0.66^{63}
	DemaTfO		3.93×10^{-6}	2.45×10^{-6}	0.60
RDE	98 wt% H ₃ PO ₄	25	1.41×10^{-6}	4.88×10^{-8}	0.65^{42}
RDE		75	6.84×10^{-6}	9.00×10^{-8}	0.64^{42}
RDE					0.62^{12}
HMRDE	50 wt% H ₃ PO ₄	25	_	_	0.48^{12}
RDE	1M Na ₂ SO ₄	25	_	_	0.62^{5}
HMRDE					0.62^{5}

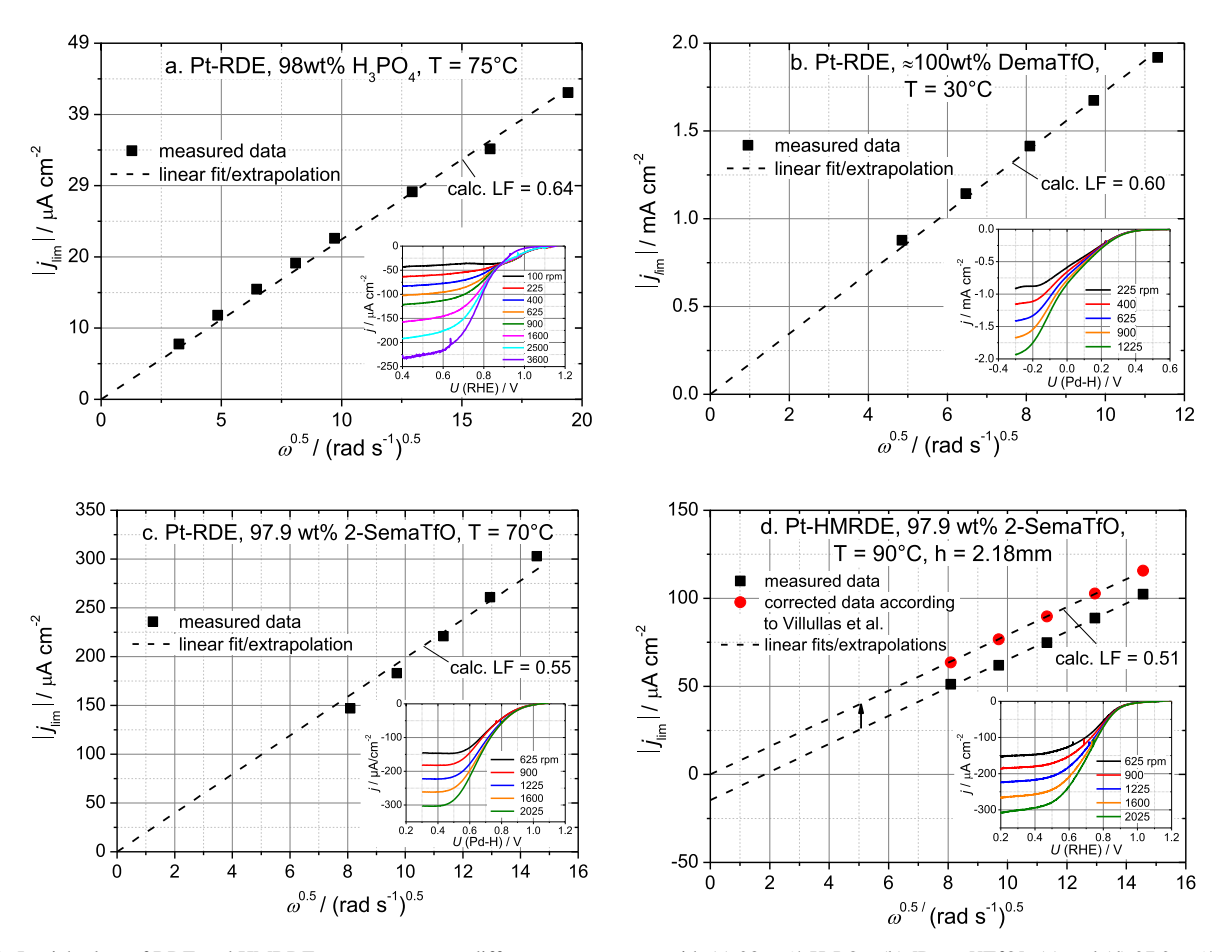


Figure 4. Levich plots of RDE and HMRDE measurements at different temperatures with (a) 98 wt% H₃PO₄; (b) [Dema][TfO]; (c) and (d) 97.9 wt% [2-Sema] [TfO]; (d) the corrected data were calculated according to Villullas et al.⁵; the inset pictures show the corresponding *U/I* curves at different rotation rates.

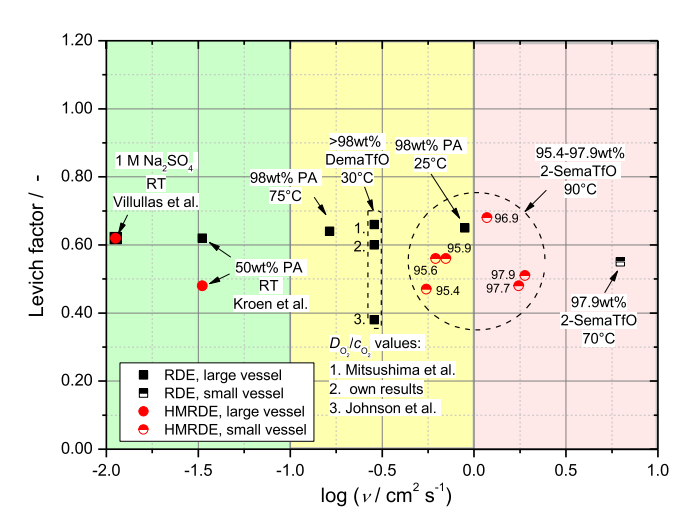


Figure 5. Plot of Levich factors vs the logarithm of the kinematic viscosity of the electrolytes; data are either fully calculated from our own experiments, calculated from our own electrochemical measurements but with D_{02}/c_{02} values taken from literature^{62,63} or completely taken from the literature^{5,12}; green = non-critical viscosity, red = critical viscosity, yellow = critical/non-critical viscosities (depending on the rotation rate); black squares = RDE measurements, red circles = HMRDE experiments; half-filled symbols = Pt vessel (3–4 ml), full symbols = glass cell (about 100 ml).

measurement vessel, i.e., either the small Pt vessel or large glass cell, is distinguished by half-filled and full symbols.

Starting at the smallest viscosities with aqueous Na_2SO_4 solution, Villullas et al.⁵ obtained LF = 0.62 for both the RDE and HMRDE

measurements and thus demonstrated the applicability of HMRDEs under these conditions. In contrast, the HMRDE experiments of Kroen et al., with 50 wt% phosphoric acid, revealed a significantly lower LF value (0.48) compared to the RDE measurements (0.62). The deviation of the LF values is surprising, as the kinematic viscosity lies within the non-critical region and lateral wetting of the HMRDE was avoided according to the authors. Conversely, the RDE experiments performed with 98 wt% H₃PO₄ at 75 °C yielded an LF much closer to the theoretical value, even though edge effects should be expected at low rpm values (see Fig. 4a).

The RDE measurements performed with [Dema][TfO], which should reveal edge effects across the entire rpm range applied (see above), indicate a general problem when calculating LFs based on Eq. 7: the accuracy of these calculations depends very much on the precision of the electrochemical experiments (limiting current densities → slope of the Levich plot!) and the measurements of the bulk parameters of the respective electrolyte. For this reason, we compared LF values based on our own $D_{\rm O2}$ and $c_{\rm O2}$ data and those taken from the literature. The lowest LF value (0.38) and largest deviation from the theoretical value is obtained with the $D_{\rm O2}$ and $c_{\rm O2}$ data of Johnson et al., 62 whereas the calculation based on the data of Mitsushima et al.63 yields an LF of 0.66, which is much closer to 0.62. The LF of 0.60 calculated from our own measurements ranges between the latter values and is closest to the theoretical value. The significant differences in D_{O2} , c_{O2} and LF can hardly be explained by different amounts of residual water, particularly as the LF values do not correlate with the water content of the [Dema][TfO] charges used by Mitsushima et al. (< 50 ppm, ⁶³), Johnson et al. (240 ppm, and in this work (4000 ppm). For 98 wt% phosphoric acid at 25 °C, an LF of 0.65 is calculated, which is almost identical to that obtained at 75 °C (see above). Once again, a Levich plot with less deviation from the values predicted by Levich's theory is obtained (not shown here), even though edge effects would be expected across the whole rpm range applied.

This is even more true for HMRDE measurements with highly viscous electrolytes such as [2-Sema][TfO]. The LF values calculated for the six mixtures of [2-Sema][TfO] and water scatter around a mean value of 0.54 ± 0.08 , which is below the theoretical value and can be explained qualitatively by the high average viscosity of these electrolytes, which is beyond the critical value. However, because the Reynolds numbers of all six [2-Sema][TfO] electrolytes are lower than the critical value, one would have expected a decrease in the LF values with decreasing water content, i.e., increasing viscosity. 50 Instead, no clear trend is observable. One explanation for this is that the edge effect proposed for RDEs may not be valid for HMRDEs, either because the pronounced intrinsic edge effect caused by the reverse flow in the perturbed area masks the RDE edge effect, or the latter one is negligible in the case of the HMRDEs. Another explanation is that the expected decrease in the LF is obscured by the large scattering of LF values. This also explains why the LF for 97.9 wt% [2-Sema][TfO] at 90 °C is not significantly higher than that for 70 °C, as one would expect. However, a definite answer cannot be given here and requires further, detailed research.

The large scattering of the LFs can be explained by the following factors: (i) errors in the determination of the bulk properties (especially $D_{\rm O2}$ and $c_{\rm O2}$); (ii) entrapment of small air bubbles, which are not visible in the opaque Pt vessel used for this experiment; (iii) a relatively narrow rpm range leading to errors in the determination of both the slope and intercept; (iv) inaccurate estimation of the meniscus height, eventually resulting in small heights close to the critical value; (v) slight lateral wetting, which may not be visible after lifting the HMRDE.

The errors described in points (i)-(iv) would result in too low or too high Levich factors, whereas point (v) would only cause an increase in the LF value. The error raised in point (i) could be minimized by using additional/alternative methods, e.g., gravimetric methods instead of chronoamperometry for the determination of the oxygen solubility. A transparent vessel would help in identifying small gas bubbles (point ii). The problem of a small rpm range (point iii) is intrinsic to rotating disk electrodes in highly viscous electrolytes and is difficult to solve: Low rotational rates lead to edge effects, while at high rpms gas bubbles might be entrapped and turbulences might occur. Whereas points (i)-(iii) are also sources of error for RDEs in viscous electrolytes, issues (iv) and (v) are specific problems of the HMRDE. The error described in point (iv) could be minimized by a more precise positioning device in combination with a transparent vessel. This would also help to identify gas bubbles (point ii). Slight lateral wetting (v) means the generation of an "electrolyte ring" with a very small height that would hardly be visible. In fact, even a height as small as 100 μ m would produce an increase in the active surface and the limiting current of 8% if a disk with a radius of 2.5 mm is used. Thus, the precise determination of mass transport currents in highly viscous electrolytes by means of an HMRDE is only possible if the above-mentioned sources of error are minimized. Moreover, a small scattering of the LF value would make visible the dependence of LF on the viscosity. This would also answer the question as to whether the critical limits proposed for RDEs are valid for HMRDEs.

Verification of the theory of Villullas et al. for viscous electrolytes.—Based on the theory presented in section 2 and in the Supplementary Material, the values of K, h_0 and k can be calculated for the six [2-Sema][TfO]/water mixtures. An interesting aspect of this is the comparison of the values obtained for viscous electrolytes (our work) and for the low viscous, aqueous electrolytes used by Villullas et al.⁵ At first, the correction term $K v^{0.5} \omega^{-0.5}$ (see Eq. S1 in Supplementary Material is available online at stacks.iop. org/JES/167/046511/mmedia) for the calculation of the effective

disk radius is reviewed in detail. For a given rotational speed, the correction term depends on the K value and the kinematic viscosity of the electrolyte. For the [2-Sema][TfO]/water mixtures, an average K value of 0.18 \pm 0.07 is obtained, which corresponds to a mean difference $h-h_0$ of 0.29 \pm 0.08 mm, with a mean h_0 value of 1.91 \pm 0.09 mm

The respective *K* value for the same height difference in the work of Villullas et al.⁵ amounts to ≈ 0.5 . Taking the different disk radii in our work (0.25 cm) and Villullas' publication (0.15 cm) into account and considering that the parameters K and k are proportional to the square of the disk radius, 5 a mean K value of 0.064 can be calculated from our data for an electrode radius of 0.15 cm. The recalculated K value is about eight times smaller than the corresponding value of Villullas et al. of ≈ 0.5 . At the same time, the square root of the kinematic viscosity increases by a factor of about 10 when using [2-Sema][TfO]/water mixtures instead of an aqueous electrolyte (see Table I). Clearly, when using a viscous electrolyte, the increase in kinematic viscosity is nearly compensated by a corresponding decrease of K. A full compensation would be merely incidental, because of measurement errors and different disk metals (Au and Pt) used in Villullas' and our work. Regarding Eq. 6d, this means that the ratio of the intercept and the slope remains virtually constant, independent of the viscosity of the electrolyte. This is confirmed by similar intercept/slope ratios of $1.35~\rm s^{-0.5}$ (this work) and $1.38~\rm s^{-0.5}$ (estimated for $h - h_0 = 0.21$ mm from Fig. 1 in Villullas et al.⁵). In other words, if the intercept/slope ratio remains constant for

In other words, if the intercept/slope ratio remains constant for the same difference in $h-h_0$ and equal disk radii, the product of K and $\nu^{0.5}$ must be constant as well, see Eq. 6d. Moreover, this means that the thickness of the perturbed layer must be virtually independent of the viscosity of the electrolyte, which contradicts the assumption of Cahan⁵ that $\delta_{\rm pl}$ has the same dimension as the hydrodynamic layer. In the latter case, one would expect a pronounced increase in $\delta_{\rm pl}$ of more than one order of magnitude if using a viscous ionic liquid like [2-Sema][TfO] instead of an aqueous electrolyte, cf. Eq. 2. This is hardly possible because $\delta_{\rm pl}$ would exceed the diameter of the disk electrode (compare $\delta_{\rm h}$ values of [2-Sema][TfO]/water mixtures in Table I). Moreover, according to Eqs. 6b to 6d, the intercept/slope ratio cannot remain constant, as the intercept increases with $\nu^{1/3}$ and the slope decreases with $\nu^{-1/6}$. In this case, one would expect an increase of the intercept/slope ratio with $\nu^{0.5}$. Because K $\nu^{0.5}$ is almost constant, it can be assumed that K is proportional to $\nu^{-0.5}$. Moreover, K is proportional to $r_0^{2.5}$ When introducing a proportionality parameter K with the dimension cm⁻¹ s^{-0.5}, independent of the viscosity and disk radius, K may be written as K = K $\nu^{-0.5}$ r_0^{2} . Then, the Eqs. S1, 6a can be formulated as follows:

$$r_{\text{eff}} = r_0 - K' \nu^{-0.5} r_0^2 \left(\frac{\nu}{\omega}\right)^{0.5} = r_0 - K' r_0^2 \omega^{-0.5}$$
 [9]

$$i_{\text{lim ,HMRDE}} = 0.62 \, n \, F \, D^{\frac{2}{3}} \, \omega^{\frac{1}{2}} \, \nu^{-\frac{1}{6}} \, C_0 \, \pi r_0^2 \times [1 - (2 \, K' r_0 \omega^{-0.5})]$$

$$intercept_{\text{HMRDE}} = -1.24 \, n \, F \, D^{\frac{2}{3}} \, \nu^{-\frac{1}{6}} \, C_0 \, \pi r_0^3 K'$$
 [11]

$$K' = -\frac{intercept_{\text{HMRDE}}}{slope_{\text{HMRDE}} \times 2r_0}$$
 [12]

The dependencies of the intercept and slope on the kinematic viscosity are now identical and thus the ratio of the intercept and slope is independent of the viscosity.

Villullas et al.⁵ introduced a parameter $k = K/(h - h_0)$ with the dimension cm⁻¹, which is more meaningful than K because it is adjusted to the actual height difference. The parameter k is regarded as a material-specific parameter that depends on the wettability of the disk surface and disk radius.⁵ Because of $K = k (h - h_0)$, both

parameters K and k should show the same dependence on the viscosity and disk radius. Thus, k may be written as:

$$k = k' v^{-0.5} r^2$$
 [13]

Here, k' is a proportionality parameter with the dimension cm⁻² s^{-0.5}, which includes not only information about the wetting properties of the specific electrode/electrolyte interface, but is independent of the kinematic viscosity of the electrolyte and disk radius. For the [2-Sema][TfO]/water mixtures, a mean k value of 6.7 ± 2.2 cm⁻¹ is obtained. The relatively high standard deviation of k is mainly caused by the error in determining the intercept of Levich plots (used for the calculation of K; see Eq. 6d) and the meniscus height. Correction for a disk radius of 0.15 cm yields a k value of 2.4 cm⁻¹, which is about ten times smaller than the k value of Villullas et al. for the system Au/1 M Na₂SO₄ + 0.005 M ferro/ferricyanide ($k \approx 22$ cm⁻¹). Again, the increase in viscosity is nearly compensated by the decrease in k. Thus, similar k' values of 121 (mean value) and 106 cm⁻² s^{-0.5} are obtained for the [2-Sema] [TfO]/water mixtures and for the aqueous electrolytes used by Villullas et al. This is illustrated in Fig. 6, where plots of K' vs h are shown for Villullas' system and for Pt/96.9 wt% [2-Sema] [TfO].

Apart from measuring errors, different k' values (or varying k values for the same viscosity and disk radius) may be explained by differences in the wetting properties of a specific electrode/electrolyte interface. Villullas et al. did not present k values for Pt electrodes, but observed smaller contact angles for Pt electrodes in comparison to the Au disks when in contact with an aqueous electrolyte. According to Villullas et al., this has been attributed to the more hydrophilic nature and stronger wetting of the Pt surface and should lead to a decrease of k, e.g., for copper disks, k values of even only half of that of Au were obtained. However, k and k' values for different electrode (and electrolyte) materials must be interpreted with care. This is because the wetting properties depend on actual surface properties like hydrophilicity under electrochemical operation, which includes the influence of potential and thus the formation of adsorbate layers or even oxides.

The question remains, however, as to why reliable and satisfactory results of mass transport can be obtained with viscous electrolytes like [Dema][TfO] and concentrated phosphoric acid, even though the thickness of the hydrodynamic layer and Reynolds number are critical and thus edge effects should arise. A definitive answer to this question cannot be given, but some possible reasons can be discussed. One aspect is the question of whether the critical values of δ_h and Re are valid for both Newtonian and non-Newtonian (power law) fluids. Equations 2 and 3 were established for the mass transport of Newtonian fluids in order to calculate δ_h and $\delta_{h, crit}$ values. However, according to Legrand et al., the critical Reynolds number of 30 is also valid for non-Newtonian fluids.⁵⁰ Because $\delta_{\rm H,crit}$ and $R_{\rm crit}$ are linked to each other—see Eqs. 5a and 5b—it can be assumed that the critical thickness of the hydrodynamic layer calculated from Eq. 2 is valid for non-Newtonian fluids as well. Hence, the above question cannot be answered by possible non-Newtonian behavior of the viscous electrolytes.

Legrand et al. determined the critical Reynolds number from plots of Sh/(Sc $^{1/3}$ Re $^{1/2}$) vs Re, with Sh and Sc as Sherwood and Schmidt numbers for the rotating disks. Above Re = 30, Sh/(Sc $^{1/3}$ Re $^{1/2}$), ratios of 0.62 were obtained, according to Levich's theory. Below the critical value, the Sh/(Sc $^{1/3}$ Re $^{1/2}$) ratio continually decreased down to values of less than 0.4. Closer inspection of Legrand's Sh/(Sc $^{1/3}$ Re $^{1/2}$) vs Re plots reveals that, depending on the electrolyte, a deviation from the 0.62 value occurred in the range of Re \approx 10–30. If the critical Reynolds number would be 10 instead of 30 for a specific electrolyte, the $\delta_{\rm h,crit}$ value would be about two times higher, i.e., $\delta_{\rm h,crit} = 2/3~d_{\rm RDE}$. This might explain the satisfactory experimental results of [Dema][TfO] and concentrated phosphoric acid at low temperatures. Indeed, $\delta_{\rm h}$ was less than two times higher than $\delta_{\rm h,crit}$ in a large part of the experimental rpm range for these electrolytes. In this case, the edge

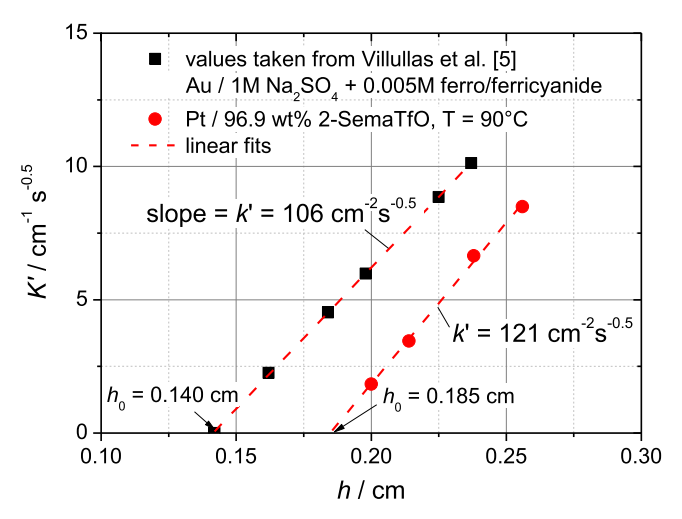


Figure 6. Plots of proportionality parameter K' vs meniscus height h; comparison of the aqueous system used by Villullas et al. 5 (Au / 1 M Na₂SO₄ + 0.005 M ferro/ferricyanide) and one of the ionic liquid systems used in this work (Pt / 96.9 wt% [2-Sema][TfO]); the slope of the linear fits is equal to the material-specific parameter k' and the zero intercept yields critical meniscus heights h_0 .

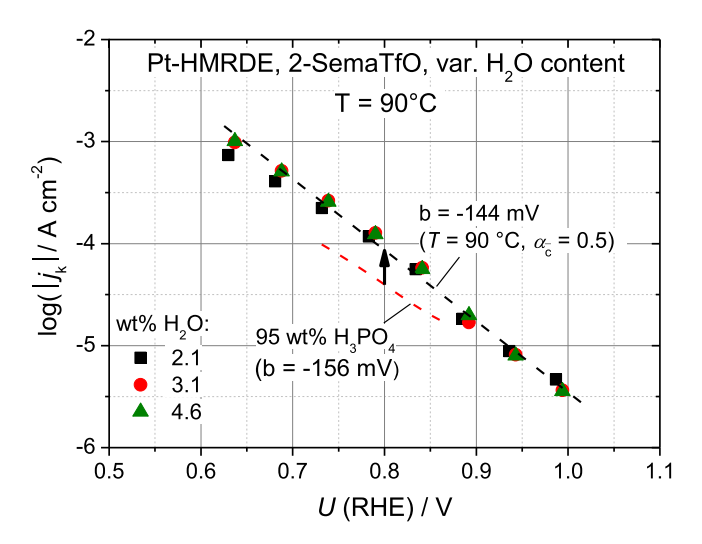


Figure 7. Tafel plots of the kinetic current density (j_k) for different water contents of [2-Sema][TfO]; j_k values calculated from Koutecký–Levich plots based on Eq. S5, see Supplementary Material; the black, broken line with arbitrary values of j_k has a slope that corresponds to the theoretical b value of -144 mV (@ T=90 °C, $\alpha=0.5$); the red, broken line shows the Tafel plot obtained with 95 wt% H_3PO_4 and a stationary Pt electrode.

effects were obviously small and have only little effect on the mass transport in front of the rotating disk. Because there is no sharp transition from uncritical to critical viscosities, the defined limit value depends on the accepted error. However, the investigation of this relationship would require more detailed experiments and is not addressed in this work.

ORR kinetics on Pt-HMRDEs in [2-Sema][TfO].—Thus far, the experimental results have shown that, in the mass transport-controlled potential range, reasonable limiting currents and Levich plots are obtained with RDEs if the viscosity of the electrolyte does not exceed the critical value by much. In the latter case, namely for viscous ionic liquids like [2-Sema][TfO] and particularly at temperatures lower than 90 °C and with small water contents, significantly smaller LF values are obtained. For the six mixtures of [2-Sema][TfO] and water at 90 °C, mass transport parameters like $j_{\rm lim}$ and LF showed considerable errors. In order to clarify whether

this also applies to smaller overpotentials, i.e., the mixed and kinetic controlled potential range, the kinetic current densities j_k of the ORR were calculated from the Koutecký-Levich analysis of the current/ potential curves of the system Pt-HMRDE/[2-Sema][TfO]+water $(90 \, ^{\circ}\text{C}, 625-2025 \, \text{rpm}, 1.7-3.6 \, \text{wt}\% \, \text{H}_2\text{O})$. In the case of HMRDEs, a modified Koutecký-Levich equation must be used⁶ (for details see third section in the Supplementary Material, Eq. S5 is available online at stacks.iop.org/JES/167/046511/mmedia).

Examples of the resulting Tafel plots are shown in Fig. 7 for three H₂O concentrations of the system [2-Sema][TfO]/water. As is apparent, the values obtained from the Koutecký-Levich analysis are close to the broken line, which corresponds to the theoretical b factor of −144 mV at 90 °C, assuming a charge transfer coefficient of 0.5. For all the investigated water concentrations, fairly linear Tafel plots with a mean Tafel slope of -147 ± 4 mV are obtained. Only at potentials lower than 0.7 V, where the current density exceeds 50% of j_{lim} do the calculated j_k values deviate from the linear function. The influence of the water content on the ORR current density in the investigated concentration range is small, although there seems to be a slight tendency towards increasing i_k with the water concentration at potentials < 0.9 V. The ORR current density at the interface of a (static) Pt wire with concentrated phosphoric acid is given for comparison¹³ (see red, broken line). It turns out that at a potential of 0.8 V, which is typical for high temperature fuel cell cathode operation, two to three times higher ORR current densities are obtained with the [2-Sema][TfO]/water mixtures. This can mainly be explained by the significantly smaller poisoning effect in the presence of the sulfonic acid-based [TfO] anions compared to phosphate ions. In any case, the analysis of the kinetic current densities proves that reliable results of electrode kinetics can be obtained with HMRDEs, even in viscous electrolytes. This is no contradiction from the deviations observed for the oxygen transport, as in the Koutecký-Levich analysis, the kinetic and limiting current densities are regarded as independent of each other. If that is the case, accurate kinetic parameters (kinetic current densities, b factors, etc.) can be obtained, independent of the particular limiting current.

Conclusions

The main goal of this study was the conducting of a suitability test of the HMRDE technique for the study of electrochemical processes in the interface of polycrystalline electrodes and viscous electrolytes, in particular for ionic liquids (IL). As an example, we investigated the oxygen transport and oxygen reduction reaction (ORR) kinetics on platinum RDEs and hanging meniscus RDEs (HMRDE) with phosphoric acid and proton-conducting ionic liquids, namely [2-Sema][TfO] and [Dema][TfO]. Based on our results, the following conclusions can be drawn:

- RDE measurements yield reasonable mass (oxygen) transport parameters, as long as the thickness of the hydrodynamic layer, $\delta_{\rm h}$, is not considerably higher than the critical limit proposed by Legrand et al., i.e., 1/3 of the disk diameter. ⁵⁰ However, our measurements with concentrated phosphoric acid and [Dema] [TfO] revealed sound results, even for δ_h values as high as $\frac{2}{3}$ of the disk diameter. This suggests that the critical $\delta_{\rm h}$ value may be somewhat higher than the value proposed in the literature.
- Additional sources of error must be considered when using viscous electrolytes such as ionic liquids. This is especially true for HMRDE experiments, where a large variation of the Levich factors is obtained. Thus, the HMRDE technique can only provide accurate values of mass transport parameters in viscous electrolytes if the experimental error is considerably reduced.
- In contrast, the HMRDE technique appears to be suitable for determining the kinetic parameters of electrochemical reactions, even in viscous electrolytes, provided that the kinetic parameters are largely independent of the mass transport.

- The question of whether the proposed RDE edge effect would also be valid for HMRDEs and/or is obscured by the intrinsic HMRDE edge effect (reverse flow of the electrolyte) is still open and requires further research. This means that extensive HMRDE measurements around the critical limit and a substantial improvement of the accuracy in determining bulk and mass transport parameters are required.
- The thickness of the perturbed layer near the edge of an HMRDE was found to be virtually independent of the viscosity. This result contradicts the assertion of Cahan that the thickness of the area of reverse flow would be of the same order of magnitude compared to the thickness of the hydrodynamic layer.⁵ Our result seems reasonable, because according to Cahan's assumption, the area of reverse flow in viscous electrolytes would be equal to or even larger than the disk area.

The hanging meniscus rotating disk electrode (HMRDE) technique is useful for avoiding leak currents that may occur with mantled (embedded) electrodes like common RDEs or microelectrodes. This applies in particular to operation at elevated temperatures >100 °C and thermal cycling. In view of this advantage and the above conclusions, it appears appropriate to use HMRDEs at temperatures much higher than 100 °C, which makes them attractive for the investigation of ionic liquids at high temperatures. At temperatures lower than 100 °C, with the exception of measurements on single crystal electrodes, RDE and microelectrode techniques appear to be advantageous because they are more straightforward and less prone to errors.

Acknowledgments

We gratefully acknowledge the preparation and Karl-Fischer titration of the electrolytes by K. Klafki and J. Stremme. We would also like to express our thanks to A. Schwaitzer (ZEA-1) for the preparation of the microelectrodes. We are obliged to C. Wood for proofreading the manuscript.

ORCID

K. Wippermann https://orcid.org/0000-0002-5489-9280

References

- 1. D. Dickertmann, F. D. Koppitz, and J. W. Schultze, *Electrochim. Acta*, 21, 967 (1976).
- 2. B. D. Cahan and H. M. Villullas, Extended Abstracts, Electrochemical Society, **88-2**, 1010 (1988).
- 3. B. D. Cahan and H. M. Villullas, J. Electroanal. Chem. Interfacial Electrochem., **307**, 263 (1991).
- 4. B. D. Cahan, H. M. Villullas, and E. B. Yeager, J. Electroanal. Chem. Interfacial Electrochem., 306, 213 (1991).
- 5. H. M. Villullas and M. L. Teijelo, J. Electroanal. Chem., 384, 25 (1995).
- H. M. Villullas and M. L. Teijelo, *J. Electroanal. Chem.*, 385, 39 (1995).
 H. M. Villullas and M. L. Teijelo, *J. Electroanal. Chem.*, 418, 159 (1996)
- 8. H. M. Villullas, V. Brunetti, and M. L. Teijelo, J. Electroanal. Chem., 437, 255 (1997).
- 9. A. Hitotsuyanagi, M. Nakamura, and N. Hoshi, *Electrochim. Acta*, **82**, 512 (2012).
- 10. M. F. Li, L. W. Liao, D. F. Yuan, D. Mei, and Y.-X. Chen, Electrochim. Acta, 110, 780 (2013)
- 11. R. Rizo, E. Herrero, and J. M. Feliu, *Phys. Chem. Chem. Phys.*, 15, 15416 (2013).
- 12. C. F. Kroen, G. E. Stoner, and S. R. Taylor, Proc. Intersoc. Energy Convers. Eng. Conf., 24, 1569 (1989).
- 13. K. Wippermann, J. Wackerl, W. Lehnert, B. Huber, and C. Korte, J. Electrochem. Soc., 163, F25 (2016).
- 14. K. Wippermann, J. Giffin, S. Kuhri, W. Lehnert, and C. Korte, Phys. Chem. Chem. Phys., 19, 24706 (2017).
- 15. K. Wippermann, J. Giffin, and C. Korte, J. Electrochem. Soc., 165, H263 (2018).
- 16. S.-Y. Lee, T. Yasuda, and M. Watanabe, J. Power Sources, 195, 5909 (2010).
- 17. A. Noda, M. A. B. H. Susan, K. Kudo, S. Mitsushima, K. Hayamizu, and M. Watanabe, J. Phys. Chem. B, 107, 4024 (2003).
- 18. D. Zhang, T. Okajima, F. Matsumoto, and T. Ohsaka, J. Electrochem. Soc., 151, D31 (2004)
- 19. H.-Y. Huang, C.-J. Su, C.-L. Kao, and P.-Y. Chen, J. Electroanal. Chem., 650, 1 (2010).
- 20. H. Munakata, T. Tashita, M. Haibara, and K. Kanamura, ECS Trans., 33, 463
- 21. A. Khan, X. Lu, L. Aldous, and C. Zhao, J. Phys. Chem. C, 117, 18334 (2013).
- 22. A. Khan and C. Zhao, ACS Sustainable Chem. Eng., 4, 506 (2016).

- S. Monaco, A. M. Arangio, F. Soavi, M. Mastragostino, E. Paillard, and S. Passerini, *Electrochim. Acta*, 83, 94 (2012).
- J. Gao, J. Liu, W. Liu, B. Li, Y. Xin, Y. Yin, J. Gu, and Z. Zou, *Int. J. Hydrogen Energy*, 37, 13167 (2012).
- Y. Tan, C. Xu, G. Chen, N. Zheng, and Q. Xie, *Energy Environ. Sci.*, 5, 6923 (2012).
- E. E. Switzer, R. Zeller, Q. Chen, K. Sieradzki, D. A. Buttry, and C. Friesen, J. Phys. Chem. C, 117, 8683 (2013).
- C. J. Allen, J. Hwang, R. Kautz, S. Mukerjee, E. J. Plichta, M. A. Hendrickson, and K. M. Abraham, *J. Phys. Chem. C*, **116**, 20755 (2012).
- 28. A. Ejigu and D. A. Walsh, J. Phys. Chem. C, 118, 7414 (2014).
- 29. J. Herranz, A. Garsuch, and H. A. Gasteiger, J. Phys. Chem. C, 116, 19084 (2012).
- D. A. Walsh, A. Ejigu, J. Smith, and P. Licence, *Phys. Chem. Chem. Phys.*, 15, 7548 (2013).
- P. Kiatkittikul, J. Yamaguchi, R. Taniki, K. Matsumoto, T. Nohira, and R. Hagiwara, J. Power Sources, 266, 193 (2014).
- R. G. Evans, O. V. Klymenko, S. A. Saddoughi, C. Hardacre, and R. G. Compton, J. Phys. Chem. B, 108, 7878 (2004).
- A. S. Barnes, E. I. Rogers, I. Streeter, L. Aldous, C. Hardacre, G. G. Wildgoose, and R. G. Compton. J. Phys. Chem. C. 112, 13709 (2008).
- S. R. Belding, E. I. Rogers, and R. G. Compton, J. Phys. Chem. C, 113, 4202 (2009).
- X.-J. Huang, E. I. Rogers, C. Hardacre, and R. G. Compton, *J. Phys. Chem. B*, 113, 8953 (2009).
- E. I. Rogers, X.-J. Huang, E. J. F. Dickinson, C. Hardacre, and R. G. Compton, *L. Phys. Chem. C* 113, 17811 (2009)
- J. Phys. Chem. C, 113, 17811 (2009).
 X.-Z. Yuan, V. Alzate, Z. Xie, D. G. Ivey, E. Dy, and W. Qu, J. Electrochem. Soc.,
- A458 (2014).
 P. Li, E. O. Barnes, C. Hardacre, and R. G. Compton, *J. Phys. Chem. C*, 119, 2716 (2015).
- T. Vainikka, M. C. Figueiredo, K. Kontturi, and L. Murtomaki, *Electrochim. Acta*, 156, 60 (2015).
- A. Khan, C. A. Gunawan, and C. Zhao, ACS Sustainable Chem. Eng., 5, 3698 (2017).
- 41. D. Pletcher, NATO ASI Ser., Ser. E, 197, 3 (1991).
- B. R. Scharifker, P. Zelenay, and J. O. M. Bockris, *J. Electrochem. Soc.*, 134, 2714 (1987).

- 43. S. Fletcher, Chem. Aust., 61, 80 (1994).
- J. Wojtowicz and B. E. Conway, J. Electroanal. Chem. Interfacial Electrochem., 13, 333 (1967).
- E. B. Yeager, P. Bindra, S. Clouser, and S. Srangapani, O₂ Reduction on Platinum Catalysts in H₃PO₄, in Electric Power Research Institute Final Report, EM-1814 (1981)
- C. L. Bentley, A. M. Bond, A. F. Hollenkamp, P. J. Mahon, and J. Zhang, *Anal. Chem.*, 85, 2239 (2013).
- 47. W. H. Smyrl and J. Newman, J. Electrochem. Soc., 118, 1079 (1971).
- Q. Dong, S. Santhanagopalan, and R. E. White, J. Electrochem. Soc., 155, B963 (2008).
- V. G. Levich, *Physicochemical hydrodynamics* (Prentice-Hall, Englewood Cliffs, N.D. (1962)
- 50. J. Legrand, E. Dumont, J. Comiti, and F. Fayolle, *Electrochim. Acta*, 45, 1791 (2000).
- I. Cornet, W. N. Lewis, and R. R. Kappesser, Trans. Inst. Chem. Eng., 47, T222 (1969).
- T. Yasuda, H. Kinoshita, M. S. Miran, S. Tsuzuki, and M. Watanabe, *J. Chem. Eng. Data*, 58, 2724 (2013).
- 53. N. N. Greenwood and A. Thompson, J. Chem. Soc., 3485 (1959).
- 54. D.-T. Chin and H. Chang, J. Appl. Electrochem., 19, 95 (1989).
- N. C. Merkel, C. Roemich, R. Bernewitz, H. Kuenemund, M. Gleiss, S. Sauer, T. J. S. Schubert, G. Guthausen, and K. Schaber, *J. Chem. Eng. Data*, 59, 560 (2014).
- K. Schrödter, G. Bettermann, T. Staffel, F. Wahl, T. Klein, and T. Hofmann, *Ullmann's Encyclopedia of Industrial Chemistry* (Wiley-VCH Verlag GmbH & Co. KGaA, Weinheim, Germany) (2000).
- D. L. Boxall, J. J. O'Dea, and R. A. Osteryoung, *J. Electrochem. Soc.*, 149, E468 (2002).
- 58. A. Giaccherini and A. Lavacchi, COMSOL Conference 2016 Munich (2016).
- D. Shoup and A. Szabo, J. Electroanal. Chem. Interfacial Electrochem., 140, 237 (1982).
- 60. J. C. Huang, R. K. Sen, and E. Yeager, J. Electrochem. Soc., 126, 786 (1979).
- 61. K. Wippermann, Y. Suo, and C. Korte, http://juser.fz-juelich.de/record/864004.
- L. Johnson, A. Ejigu, P. Licence, and D. A. Walsh, J. Phys. Chem. C, 116, 18048 (2012).
- S. Mitsushima, Y. Shinohara, K. Matsuzawa, and K.-I. Ota, *Electrochim. Acta*, 55, 6639 (2010).
- 64. H. M. Villullas and M. L. Teijelo, J. Appl. Electrochem., 26, 353 (1996).